Fast adiabatic preparation of multisqueezed states by jumping along the path

Chuan Chen,[1] Jian-Yu Lu,[1] Xu-Yang Chen,[1,*] and Zhen-Yu Wang[1,2,†]

[1]*Key Laboratory of Atomic and Subatomic Structure and Quantum Control (Ministry of Education), Guangdong Basic Research Center of Excellence for Structure and Fundamental Interactions of Matter, School of Physics, South China Normal University, Guangzhou 510006, China*

[2]*Guangdong Provincial Key Laboratory of Quantum Engineering and Quantum Materials, Guangdong–Hong Kong Joint Laboratory of Quantum Matter, South China Normal University, Guangzhou 510006, China*

(Received 20 March 2024; accepted 6 June 2024; published 1 July 2024)

Multisqueezed states, also known as generalized squeezed states, are valuable quantum non-Gaussian resources, because they can feature nonclassical properties such as large phase-space Wigner negativities. In this paper, we introduce a shortcuts to adiabaticity (STA) method for the fast preparation of multisqueezed states. In contrast to previous STA methods, which rely on the use of counterdiabatic control to suppress unwanted nonadiabatic effects, our method simplifies the process and accelerates state preparation by selecting an appropriate sampling along a quantum evolution path. We demonstrate the high fidelity and fast preparation of multisqueezed states, as well as hybrid entangled states between a bosonic mode and a qubit.

DOI: 10.1103/PhysRevA.110.012601

I. INTRODUCTION

Quantum adiabatic control is a fundamental concept in quantum mechanics [1–3], which implies that a physical system can be kept in its instantaneous eigenstates by applying a slowly varying control field. This facilitates various robust preparations of quantum states, such as coherent and squeezed states [4–7].

However, slow evolution, which is required in the traditional adiabatic approximation [1], makes the quantum system more susceptible to decoherence. To reduce the effects of decoherence, shortcuts to adiabaticity (STA) methods [8–17] have been developed to accelerate the adiabatic evolution. By the use of counterdiabatic driving fields to cancel out the nonadiabatic effects of the original Hamiltonian, STA schemes achieve the same outcome as traditional quantum adiabatic methods in a much shorter time.

Despite their great success, these STA methods [8–17] necessitate counterdiabatic driving, which is not always feasible or practical, due to the potential requirement of experimental resources that are hard to access [13–15]. Furthermore, counterdiabatic control fields also change the eigenstates of the original Hamiltonian and potentially introduce additional control errors, which might cause the quantum system to deviate from the intended evolution path. These factors make it difficult to design a robust STA method that can withstand control errors.

To address the problems mentioned above, the shortcut to adiabaticity by modulation (STAM) method has been proposed [18]. STAM is based on the necessary and sufficient condition of quantum adiabatic evolution [19,20]. It eliminates the nonadiabatic effects by dynamically adjusting the Hamiltonian parameters, without the need of auxiliary driving. Therefore, STAM method provides a new approach to construct parametrized Hamiltonians for adiabatic control [21,22] and new insights to manipulate quantum systems and sensing [23,24].

Here we develop a STAM method to prepare multisqueezed states [25–30]. Multisqueezed states, the higher-order generalization of coherent (first order) and squeezed states (second order) [31–33], exhibit remarkable non-Gaussian properties for third order and beyond, such as large phase-space Wigner negativities, interference, and enhanced squeezing [25–30]. These unique characteristics have made them considered as strictly quantifiable and valuable non-Gaussian resources in quantum information technology [34–39], despite initial beliefs that they were physically impossible [25]. However, subsequent theoretical analyses demonstrated the generation of multisqueezed states via spontaneous parametric down-conversion [27,28], with recent experimental realization for the third order of multisqueezed states [34].

The paper is organized as follows. In Sec. II, we construct our STAM method and show superior performance of our method over traditional adiabatic control in the preparation of multisqueezed states. In Sec. III, we extend our method to the preparation of hybrid entangled states. We draw our conclusions in Sec. IV.

II. PREPARATION OF MULTISQUEEZED STATES

Consider a bosonic system initially prepared in one of the Fock states, $|n\rangle$, which is an eigenstate of the free bosonic

*Contact author: 2022010138@m.scnu.edu.cn
†Contact author: zhenyu.wang@m.scnu.edu.cn

Hamiltonian ($\hbar = 1$):

$$H = \omega_c a^\dagger a = \sum_{n=0}^{\infty} n\omega_c |n\rangle\langle n|, \tag{1}$$

where a ($a^\dagger$) represents the annihilation (creation) operator and ω_c is the angular frequency of the bosonic mode.

We aim to adiabatically prepare the state $|n_J(\Theta)\rangle$ with

$$|n_J(\lambda)\rangle \equiv e^{-iG_J\lambda}|n\rangle \tag{2}$$

by the change of the dimensionless parameter $\lambda \equiv \lambda(t)$ which is a monotonic function with respect to the time t. The parameter changes from $\lambda(0) = 0$ to $\lambda(T) = \Theta$ for a total evolution time T. We use the Jth-order bosonic interactions

$$G_J = i[\varepsilon(a^\dagger)^J - \varepsilon^* a^J], \tag{3}$$

where J is a positive integer and ε is a complex number, for the preparation of multisqueezed states. Note that the matrix elements of G_J satisfy

$$g_{n,m} \equiv \langle n|G_J|m\rangle = \langle n_J(\lambda)|i\frac{d}{d\lambda}|m_J(\lambda)\rangle. \tag{4}$$

The Hamiltonian corresponding to multisqueezed states for adiabatic control reads

$$H_J(\lambda) = e^{-iG_J\lambda} H e^{iG_J\lambda} = \sum_{n=0}^{\infty} E_n |n_J(\lambda)\rangle\langle n_J(\lambda)|, \tag{5}$$

where $E_n = n\omega_c$.

When $J = 1$, $e^{-iG_1\lambda}$ is a displacement operator, and it gives rise to the first-order parametrized Hamiltonian $H_1(\lambda)$ for the bosonic mode:

$$\begin{aligned} H_1(\lambda) &= e^{-iG_1\lambda} H e^{iG_1\lambda} \\ &= \omega_c a^\dagger a - \lambda\omega_c(\varepsilon a^\dagger + \varepsilon^* a) + \omega_c|\lambda\varepsilon|^2, \end{aligned} \tag{6}$$

where the last term $\omega_c|\lambda\varepsilon|^2$ can be dropped out.

When $J = 2$, $e^{-iG_2\lambda}$ corresponds to a squeezing operator with $\varepsilon = re^{i\vartheta}$ by the use of real parameters r and ϑ. This transforms the original Hamiltonian into

$$\begin{aligned} H_2(\lambda) &= e^{-iG_2\lambda} H e^{iG_2\lambda} \\ &= \omega_c[a^\dagger a \cosh^2(2\lambda r) + aa^\dagger \sinh^2(2\lambda r) \\ &\quad - (a^2 e^{-i\vartheta} + \text{H.c.}) \sinh(2\lambda r)\cosh(2\lambda r)]. \end{aligned} \tag{7}$$

In traditional quantum adiabatic control, one slowly varies λ from $\lambda = 0$ to Θ, and in the infinitely slow limit, the initial state $|n_J(0)\rangle = |n\rangle$ will evolve to $|n_J(\Theta)\rangle$. While this adiabatic control has a strong robustness against amplitude fluctuation of the control fields, the long control time limits its application, e.g., due to the short coherence time of the quantum system. Here we employ the STAM method [18], which is originated from the theory of the necessary and sufficient condition of quantum adiabatic evolution [19], to prepare the target state $|n_J(\Theta)\rangle$ with unit fidelity in a fast and robust manner.

According to Ref. [19], the evolution operator $U = \mathcal{T} e^{-i\int_0^t H_J dt'}$ (where $\mathcal{T}$ represents time ordering) driven by H_J can be decomposed as

$$U = U_{\text{adia}} U_{\text{err}}, \tag{8}$$

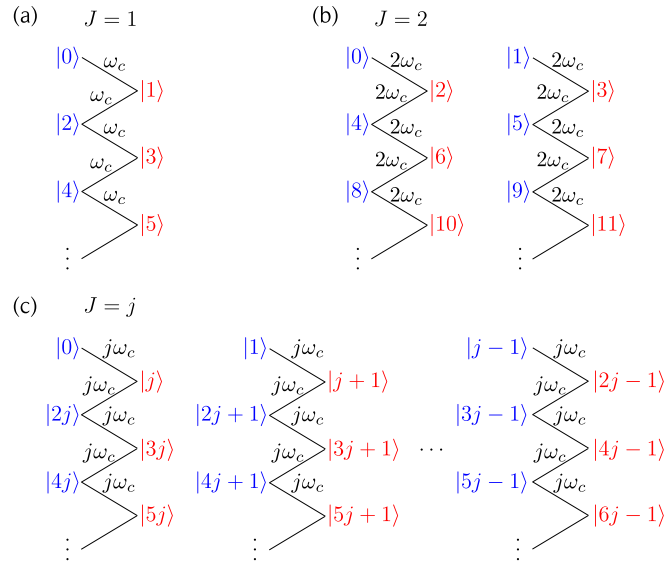

FIG. 1. Connection of all the Fock states $|n\rangle$ and $|m\rangle$ with $g_{n,m} \neq 0$ forming a graph for each given value of J. For the G_J given by Eq. (3), all the states are divided into two groups $\mathcal{R}$ (in red color) and $\mathcal{B}$ (in blue color) with only states of distinct groups being connected. For the Hamiltonian Eq. (5) the energy differences between each pair of the connected states are $J\omega_c$.

where

$$U_{\text{adia}}(\lambda) = \sum_{n=0}^{\infty} e^{-i\varphi_n} |n_J(\lambda)\rangle\langle n_J(0)| \tag{9}$$

describes the desired ideal adiabatic evolution. Since $g_{n,n} = 0$ for all n [see Eqs. (3) and (4)], each φ_n in Eq. (9) is the accumulated dynamic phase for the nth state. Meanwhile, using the path ordering $\mathcal{P}$ with respect to λ in a way similar to the time ordering, the nonadiabatic evolution reads

$$U_{\text{err}}(\lambda) = \mathcal{P} e^{i\int_0^\lambda W(\lambda')d\lambda'}, \tag{10}$$

where

$$W(\lambda) = \sum_{n\neq m} F_{n,m}(\lambda) g_{n,m} |n\rangle\langle m|, \tag{11}$$

with $F_{n,m}(\lambda) = e^{i[\varphi_n(\lambda) - \varphi_m(\lambda)]}$.

In the following we describe how to choose a functional form of $\lambda(t)$ such that all nonadiabatic effects vanish (i.e., $U_{\text{err}} = I$).

The quantities $g_{n,m}$ with nonzero values form the graphs in Fig. 1, where the Fock states $|n\rangle$ and $|m\rangle$ are either connected ($g_{n,m} \neq 0$) or disconnected ($g_{n,m} = 0$). In our case, only

$$g_{n+J,n} = i\varepsilon\sqrt{\frac{(n+J)!}{n!}} \tag{12}$$

and $g_{n,n+J} = g^*_{n+J,n}$ with $n \geqslant 0$ have nonzero values. An important property of these graphs is that all the Fock states can be divided into two groups: group $\mathcal{R}$ and group $\mathcal{B}$, illustrated in red and blue colors in Fig. 1, respectively. Additionally, only states from different groups can be connected. Therefore, if we keep the dynamic phases $\varphi_n(\lambda) = 2k_n(\lambda)\pi$ for $n \in \mathcal{B}$ while $\varphi_m(\lambda) = k_m(\lambda)\pi + \pi$ for $m \in \mathcal{R}$ with both $k_n(\lambda)$ and

$k_m(\lambda)$ being integers along the path, we can write

$$W(\lambda) = F(\lambda)\sum_{n\neq m} g_{n,m}|n\rangle\langle m|, \tag{13}$$

with a common $F(\lambda) \in \{+1, -1\}$. In this manner, $W(\lambda)$ at different λ commute and hence $U_{\rm err}(\lambda) = e^{i\int_0^\lambda W(\lambda')d\lambda'}$, where the path ordering has been removed. All nonadiabatic errors are eliminated at the end of the evolution time T, i.e., $U_{\rm err}(\Theta) = I$ when

$$\int_0^\Theta F(\lambda)d\lambda = 0. \tag{14}$$

We achieve these by applying $H_J(\lambda)$ [Eq. (5)] at N equally spaced points of the parameter $\lambda = \lambda_k$ subsequently with $k = 1, 2, \ldots, N$. Here

$$\lambda_k = \frac{\Theta}{2N}(2k-1). \tag{15}$$

The control at each λ_k has a time duration $t_p = \pi/(J\omega_c)$ such that each bosonic control pulse

$$P_k \equiv e^{-iH_J(\lambda_k)t_p} \tag{16}$$

introduces a sign change to $F(\lambda)$ at $\lambda = \lambda_k$, because the directly connected states in Fig. 1 have an energy difference of $J\omega_c$. That is, $F(\lambda) = (-1)^k$ for $\lambda \in [\lambda_k, \lambda_{k+1})$ with $\lambda_0 \equiv 0$ and $\lambda_{N+1} \equiv \Theta$. Since the sequence Eq. (15) satisfies Eq. (14), we have $U_{\rm err}(\Theta) = I$ at the end of the evolution, i.e.,

$$U(\Theta) = P_N P_{N-1}\cdots P_2 P_1 = U_{\rm adia}(\Theta). \tag{17}$$

Because $\int_0^{\Theta_k} F(\lambda)d\lambda = 0$ for any

$$\Theta_k \equiv k\Theta/N,\ (k = 0, 1, 2, \ldots, N) \tag{18}$$

we also achieve the target adiabatic evolution perfectly without any nonadiabatic errors (i.e., $U = U_{\rm adia}$) at all these parameter points $\lambda = \Theta_k$ $(k = 1, 2, \ldots, N)$.

The bosonic control pulse P_k [Eq. (16)] for the Gaussian cases (i.e., $J = 1, 2$) can be implemented in various systems [7,40]. For the non-Gaussian cases where $J \geqslant 3$, the realization of the control Hamiltonian $H_J(\lambda)$ is more challenging. A way to implement P_k is to use the composite pulse

$$P_k = e^{-iG_J\lambda_k}e^{-i\omega_c a^\dagger a t_p}e^{iG_J\lambda_k}, \tag{19}$$

where the transformations $e^{-iG_J\lambda_k}$ and $e^{iG_J\lambda_k}$ can be realized by the protocol in Ref. [38], e.g., in strongly coupled superconducting qubits and microwave resonators [41–44].

Our method avoids the long evolution time required by the traditional adiabatic methods that use slowly varying Hamiltonians. We can generate a Jth-order bosonic quantum state from the vacuum state $|0\rangle$ or other initial states, by applying the control sequence Eq. (17).

A physical picture of how the multisqueezed state is prepared by our method is provided in Fig. 2 by considering the case of $J = 1$ and the initial state being the vacuum state $|0\rangle$ (which is a coherent state). As illustrated in Fig. 2, during each control pulse P_k the state (which remains a coherent state) rotates clockwise around the point $\lambda_k\varepsilon$ with the radius $|(\Theta_{k-1} - \lambda_k)\varepsilon|$ and an angular frequency ω_c in the phase space as [45]

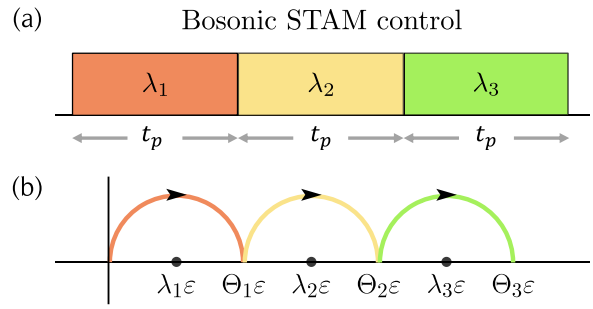

FIG. 2. STAM method for fast adiabatic control of bosonic states. (a) Control sequence for the bosonic mode. (b) The evolution trajectories of the coherent state in the phase space under the control sequence illustrated in (a).

$$e^{-iH_1(\lambda_k)t}|\Theta_{k-1}\varepsilon\rangle = |\Phi(t)\varepsilon\rangle e^{-i\theta}, \tag{20}$$

where $\Phi(t) = (\Theta_{k-1} - \lambda_k)e^{-i\omega_c t} + \lambda_k$ and the global phase θ can be neglected. When $t = t_p$, the pulse P_k is complected and it transforms the coherent state $|\Theta_{k-1}\varepsilon\rangle$, which corresponds to the ground state of $H_1(\Theta_{k-1})$, into the ground state of $H_1(\Theta_k)$.

To demonstrate that our method is much faster than traditional techniques for achieving the same outcome, in Figs. 3 and 4, we compare our STAM method with the traditional adiabatic control which uses a continuous variation of parameters, for $J = 1$ and 2, respectively. The results were simulated by using QUTIP [46,47]. Figure 3 shows the fidelity of coherent-state preparation during the control for $|\Theta\varepsilon = 20\rangle$. Our STAM method provides a much faster and much higher fidelity than the traditional adiabatic control. In Fig. 3, a fidelity of 100% can be reached within 0.5 μs by using our method, while for the traditional adiabatic control, the time for a fidelity higher than 95% is approximately 5 μs, an order of magnitude longer than the time used in our method. Note that our method performs much better than the traditional adiabatic control when the amplitude Θ is larger, since the time required in our method is a fixed pulse duration t_p while the traditional adiabatic control needs more time for a larger Θ. Similarly, Fig. 4 demonstrates the advantages of our STAM method for the preparation of squeezed vacuum state $|n = 0, \xi = 3i\rangle$. These results indicate that the STAM method can achieve the target states in a much shorter time than the traditional adiabatic control.

The idea of our method can be generalized to other quantum systems. In the following section we demonstrate the preparation of entangled states for a hybrid quantum system consisting of a qubit and a bosonic mode using our method.

III. PREPARATION OF HYBRID ENTANGLED STATES

In this section, we consider a hybrid system consisting of a bosonic mode and a qubit with the Hamiltonian

$$H_1'(\lambda) = \omega_c a^\dagger a - \lambda\omega_c(a^\dagger + a)\sigma_x, \tag{21}$$

where $\sigma_x = |e\rangle\langle g| + |g\rangle\langle e|$ with $\{|e\rangle, |g\rangle\}$ being the qubit states. This type of interaction could be realized across various platforms, including superconducting circuits [40,48–51], trapped atoms [52–55], and neutral atoms [56,57].

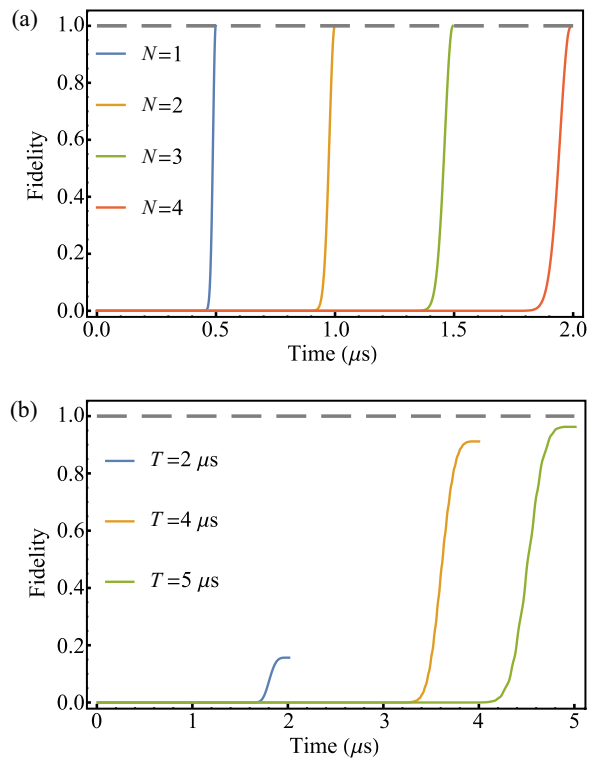

FIG. 3. Fidelity of the evolved state to the target coherent state during the control with $J = 1$. (a) The results of our STAM method for different number N of control pulses. (b) The results of the traditional adiabatic control for different total evolution time T, with a continuous variation of the control parameter $\lambda(t) = A\exp[-B(t/T-1)^2] - C$, where $A = 20.377$, $B = 4$, $C = 0.376\,974$. Here the parameters $\omega_c = 2\pi \times 1\,\mathrm{MHz}$, $\varepsilon = 1$, and $\Theta = 20$.

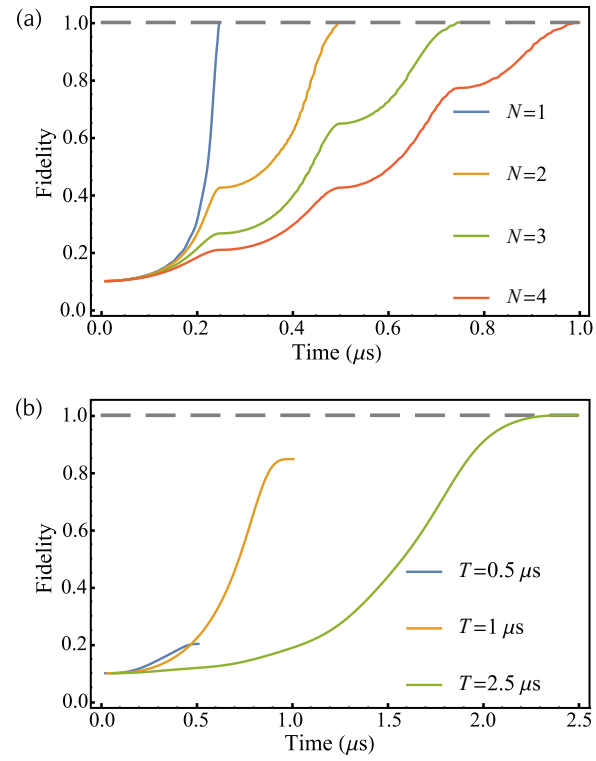

FIG. 4. Fidelity of the evolved state to the target squeezed state during the control with $J = 2$. (a) The results of our STAM method for different number N of control pulses. (b) The results of the traditional adiabatic control for different total evolution time T, with a continuous variation of the control parameter $\lambda(t) = A\exp[-B(t/T-1)^2] - C$, where $A = -0.509\,165$, $B = 4$, $C = -0.009\,164\,97$. Here $\omega_c = 2\pi \times 1\,\mathrm{MHz}$, $\varepsilon = 3i$, and $\Theta = -0.5$.

Our goal is to prepare a hybrid entangled state of the form

$$|\psi\rangle_{AB} = \frac{1}{\sqrt{2}}(|\alpha\rangle_A|+\rangle_B \pm |-\alpha\rangle_A|-\rangle_B), \tag{22}$$

where $|\pm\alpha\rangle$ represent the coherent states of the bosonic mode and $|\pm\rangle = \frac{1}{\sqrt{2}}(|e\rangle \pm |g\rangle)$ are the eigenstates of the Pauli matrix σ_x. This pure state is known as the Schrödinger-cat state [48–50,52,53,55,58–60].

A. STAM without qubit control

Regarding the states $|\pm\rangle$ of the qubit, the bosonic Hamiltonian Eq. (21) becomes

$$H_\pm(\lambda) = \omega_c a^\dagger a \mp \lambda\omega_c(a^\dagger + a), \tag{23}$$

which corresponds to Eq. (6) with $\varepsilon = 1$.

Therefore, according to the theory in Sec. II, applying the Hamiltonian $H_1'(\lambda_k)$ in Eq. (21) for a time duration $t_p = \pi/\omega_c$ would generate the pulse

$$P_k' = e^{-iH_+(\lambda_k)t_p}|+\rangle\langle+| + e^{-iH_-(\lambda_k)t_p}|-\rangle\langle-|, \tag{24}$$

which transforms the given initial state $|0\rangle|g\rangle$ to a hybrid entangled state

$$|\psi\rangle = \frac{1}{\sqrt{2}}(|\Theta_k\rangle|+\rangle - |-\Theta_k\rangle|-\rangle). \tag{25}$$

For the STAM illustrated in Fig. 5, we achieve the target hybrid entangled state

$$|\psi_{\mathrm{target}}\rangle = \frac{1}{\sqrt{2}}(|\Theta\rangle|+\rangle - |-\Theta\rangle|-\rangle). \tag{26}$$

We first consider the evolution of the von Neumann entanglement entropy [61–63] between the bosonic mode and the qubit during the STAM control. The von Neumann entanglement entropy is calculated as $\mathcal{S}(\rho_A) = -\mathrm{Tr}[\rho_A \log_2(\rho_A)]$, where $\rho_A = \mathrm{Tr}_B(\rho_{AB})$ and $\rho_B = \mathrm{Tr}_A(\rho_{AB})$ represent the

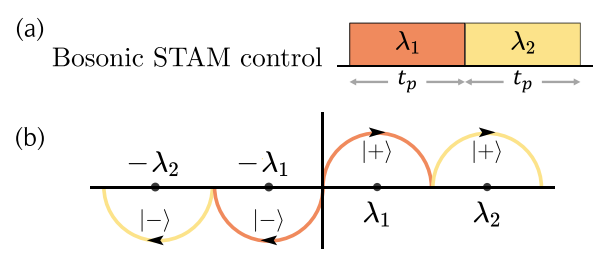

FIG. 5. Preparation of the hybrid entangled state by STAM control on a bosonic mode coupled with a qubit. (a) Control sequence for bosonic STAM. (b) Evolution of the coherent state under the control sequence illustrated in (a) is conditional to the qubit states $|+\rangle$ and $|-\rangle$.

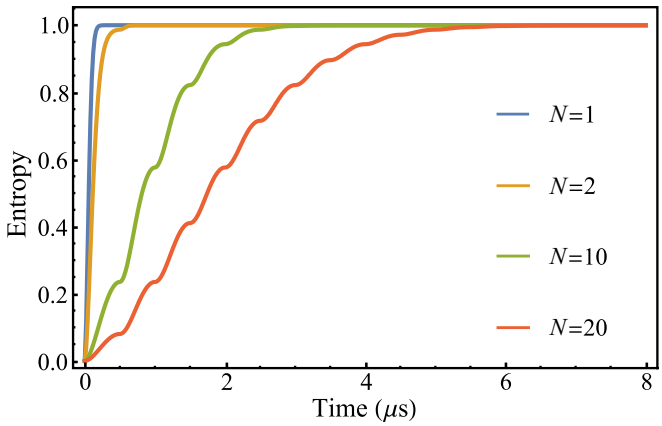

FIG. 6. Entanglement entropy evolution of the hybrid entangled state using the STAM method illustrated in Fig. 5, for different pulse number N, $\Theta = 2$, and $\omega_c = 2\pi \times 1$ MHz.

reduced density matrices for each partition [61–63]. As Eq. (22), here we refer to the bosonic mode (qubit) as the subsystem A (B). For the given final state $|\psi_{\text{target}}\rangle$ with $\Theta = 2$ in Eq. (26), Fig. 6 shows the evolution of the von Neumann entanglement entropy. The entanglement between the bosonic mode and the qubit can reach its maximum in a short time.

In Fig. 7 we further demonstrate the fidelity between the target state, Eq. (26), and the prepared state using the STAM sequence in Fig. 5. The simulated results show that our STAM sequence gives a high fidelity of the state preparation. The robustness of the sequence against pulse errors is better for a larger number N of pulses.

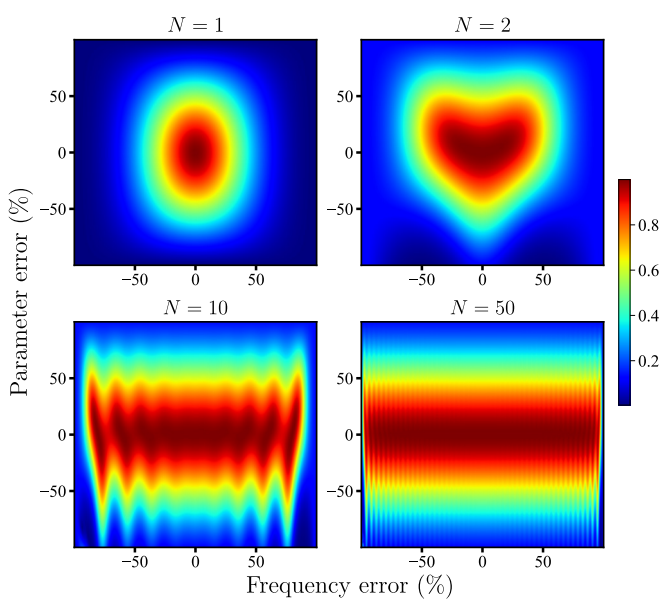

FIG. 7. Fidelity of hybrid entangled state preparation via the STAM control illustrated in Fig. 5 for various numbers N of bosonic control pulses when there are static relative fluctuations to the ideal sequence parameters λ_k [Eq. (15)] and the ideal frequency $\omega_c = 2\pi \times 100$ MHz. Here $\Theta = 2$.

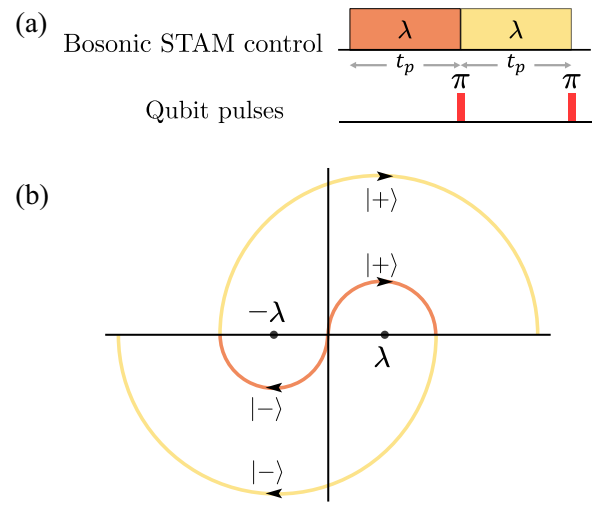

FIG. 8. Large hybrid entangled state realized by synchronized STAM control and qubit control. (a) Bosonic STAM and qubit control sequence. (b) The control sequence illustrated in (a) amplifies the trajectories of the coherent state evolution.

B. STAM with qubit control

We note that the STAM sequence in Fig. 5 restricts the possibility of preparing coherent states with an arbitrarily large Θ, because of the limited values of λ in the Hamiltonian. To address this challenge, we apply a π pulse on the qubit after each STAM pulse on the bosonic mode [see Fig. 8(a)], following a similar idea in Ref. [55]. Each qubit π pulse swaps the qubit states $|+\rangle$ and $|-\rangle$ and hence realizes the transformation $\sigma_x \to -\sigma_x$. After the application of k qubit π pulses, the Hamiltonian Eq. (21) becomes

$$H_I = \omega_c a^\dagger a - (-1)^k \lambda \omega_c (a^\dagger + a)\sigma_x. \tag{27}$$

As illustrated in Fig. 8, each qubit π pulse swaps the qubit states $|+\rangle$ and $|-\rangle$ and hence the rotating centers of the conditional bosonic evolution. Consequently, the achieved value $\Theta = 2N\lambda$ of the target state [Eq. (26)] can be arbitrarily large by increasing the number of bosonic pulses N while keeping parameter fixed, i.e., $\lambda_k \equiv \lambda$ (see Fig. 8). To enhance the robustness of the control on the qubit, we apply the qubit control Hamiltonian $H_{\text{ctrl}} = (-1)^k \frac{\Omega}{2}\sigma_z$ for the kth qubit π pulse, where the alternation of the sign mitigates potential amplitude fluctuation of the control on the qubit.

Figure 9 illustrates the simulated fidelity between the prepared state with the target states $|\psi_{\text{target}}\rangle$ [Eq. (26)] using the sequence in Fig. 8. The results show that one can reliably prepare the target state $|\psi_{\text{target}}\rangle$ with increasing values of $\Theta = 2N\lambda$. The state fidelity remains very high even with a relatively large static error in the qubit control $\Omega \to (1+\delta)\Omega$. Even when $N = 50$ and the error reaches $\delta = \pm 25\%$, the fidelity still remains above 90%.

IV. CONCLUSION AND OUTLOOK

In summary, we have proposed a STAM method to greatly speed up the adiabatic preparation of the multisqueezed states of a bosonic mode as well as the entanglement of these

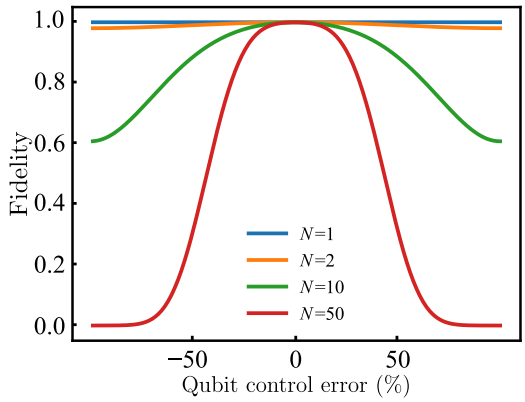

FIG. 9. Fidelity of hybrid entangled state preparation via the STAM with qubit control illustrated in Fig. 8 as a function of control error δ for various numbers N of bosonic pulses. The control amplitude $(1+\delta)\Omega$ of the qubit control has a static fluctuation with respect to the ideal one $\Omega = 2\pi \times 50\,\mathrm{MHz}$. Here $\omega_c = 2\pi \times 100\,\mathrm{kHz}$ and $\lambda = 0.05$.

states with a qubit. Our STAM method achieves the adiabatic speedup by dynamically adjusting the Hamiltonian parameters such that the nonadiabatic effects are coherently eliminated. Using our method, the target multisqueezed states can be prepared in a short finite time, e.g., less than 10% of the time required in the traditional adiabatic control as demonstrated by our numerical simulations. For the case of Schrödinger-cat state preparation in a hybrid system of a qubit and a bosonic mode, we show linear increase of the amplitude of the Schrödinger-cat state with the number of pulses. This enables fast preparation of arbitrarily high amplitude entangled multisqueezed states. The STAM method has some intrinsic robustness against some kinds of errors. The robustness of our method could be further enhanced by numerical optimization methods such as the gradient ascent pulse engineering algorithm [64,65] and other advanced techniques such as enhanced shortcuts to adiabaticity methods as discussed in recent research [66–69].

ACKNOWLEDGMENTS

This work was supported by National Natural Science Foundation of China (Grant No. 12074131), the Natural Science Foundation of Guangdong Province (Grant No. 2021A1515012030), and National College Student Innovation and Entrepreneurship Training Program (Grant No. 202310574055).

C.C. and J.-Y.L. contributed equally to this work.

[1] A. Messiah, *Quantum Mechanics* (North-Holland, Amsterdam, 1961), Vol. 2.

[2] M. V. Berry, Quantal phase factors accompanying adiabatic changes, Proc. R. Soc. A **392**, 45 (1984).

[3] T. Albash and D. A. Lidar, Adiabatic quantum computation, Rev. Mod. Phys. **90**, 015002 (2018).

[4] S.-B. Zheng, Generation of atomic and field squeezing by adiabatic passage and symmetry breaking, Phys. Rev. A **86**, 013828 (2012).

[5] C. Leroux, L. C. G. Govia, and A. A. Clerk, Enhancing cavity quantum electrodynamics via antisqueezing: Synthetic ultrastrong coupling, Phys. Rev. Lett. **120**, 093602 (2018).

[6] J. Chen, D. Konstantinov, and K. Mølmer, Adiabatic preparation of squeezed states of oscillators and large spin systems coupled to a two-level system, Phys. Rev. A **99**, 013803 (2019).

[7] U. L. Andersen, T. Gerhring, C. Marquardt, and G. Leuchs, 30 years of squeezed light generation, Phys. Scr. **91**, 053001 (2016).

[8] M. Demirplak and S. A. Rice, Adiabatic population transfer with control fields, J. Phys. Chem. A **107**, 9937 (2003).

[9] M. V. Berry, Transitionless quantum driving, J. Phys. A **42**, 365303 (2009).

[10] X. Chen, I. Lizuain, A. Ruschhaupt, D. Guéry-Odelin, and J. G. Muga, Shortcut to adiabatic passage in two- and three-level atoms, Phys. Rev. Lett. **105**, 123003 (2010).

[11] E. Torrontegui, S. Ibáñez, S. Martínez-Garaot, M. Modugno, A. del Campo, D. Guéry-Odelin, A. Ruschhaupt, X. Chen, and J. G. Muga, Shortcuts to adiabaticity, Adv. At. Mol. Opt. Phys. **62**, 117 (2013).

[12] D. Guéry-Odelin, A. Ruschhaupt, A. Kiely, E. Torrontegui, S. Martínez-Garaot, and J. G. Muga, Shortcuts to adiabaticity: Concepts, methods, and applications, Rev. Mod. Phys. **91**, 045001 (2019).

[13] M. G. Bason, M. Viteau, N. Malossi, P. Huillery, E. Arimondo, D. Ciampini, R. Fazio, V. Giovannetti, R. Mannella, and O. Morsch, High-fidelity quantum driving, Nat. Phys. **8**, 147 (2012).

[14] A. Baksic, H. Ribeiro, and A. A. Clerk, Speeding up adiabatic quantum state transfer by using dressed states, Phys. Rev. Lett. **116**, 230503 (2016).

[15] B. B. Zhou, A. Baksic, H. Ribeiro, C. G. Yale, F. J. Heremans, P. C. Jerger, A. Auer, G. Burkard, A. A. Clerk, and D. D. Awschalom, Accelerated quantum control using superadiabatic dynamics in a solid-state lambda system, Nat. Phys. **13**, 330 (2017).

[16] Y.-X. Du, Z.-T. Liang, Y.-C. Li, X.-X. Yue, Q.-X. Lv, W. Huang, X. Chen, H. Yan, and S.-L. Zhu, Experimental realization of stimulated Raman shortcut-to adiabatic passage with cold atoms, Nat. Commun. **7**, 12479 (2016).

[17] X.-K. Song, F. Meng, B.-J. Liu, D. Wang, L. Ye, and M.-H. Yung, Robust stimulated Raman shortcut-to-adiabatic passage with invariant-based optimal control, Opt. Express **29**, 7998 (2021).

[18] Y. Liu and Z.-Y. Wang, Shortcuts to adiabaticity with inherent robustness and without auxiliary control, arXiv:2211.02543.

[19] Z.-Y. Wang and M. B. Plenio, Necessary and sufficient condition for quantum adiabatic evolution by unitary control fields, Phys. Rev. A **93**, 052107 (2016).

[20] K. Xu, T. Xie, F. Shi, Z.-Y. Wang, X. Xu, P. Wang, Y. Wang, M. B. Plenio, and J. Du, Breaking the quantum adiabatic speed limit by jumping along geodesics, Sci. Adv. **5**, eaax3800 (2019).

[21] W. Zheng, J. Xu, Z. Wang, Y. Dong, D. Lan, X. Tan, and Y. Yu, Accelerated quantum adiabatic transfer in superconducting qubits, Phys. Rev. Appl. **18**, 044014 (2022).

[22] M. Gong, M. Yu, R. Betzholz, Y. Chu, P. Yang, Z. Wang, and J. Cai, Accelerated quantum control in a three-level system by jumping along the geodesics, Phys. Rev. A **107**, L040602 (2023).

[23] S. Xu, C. Xie, and Z.-Y. Wang, Enhancing electron-nuclear resonances by dynamical control switching, Phys. Rev. A **109**, L020601 (2024).

[24] K. Zeng, X. Yu, M. B. Plenio, and Z.-Y. Wang, Wide-band unambiguous quantum sensing via geodesic evolution, Phys. Rev. Lett. **132**, 250801 (2024).

[25] R. A. Fisher, M. M. Nieto, and V. D. Sandberg, Impossibility of naively generalizing squeezed coherent states, Phys. Rev. D **29**, 1107 (1984).

[26] M. Hillery, M. S. Zubairy, and K. Wódkiewicz, Squeezing in higher order nonlinear optical processes, Phys. Lett. A **103**, 259 (1984).

[27] S. L. Braunstein and R. I. McLachlan, Generalized squeezing, Phys. Rev. A **35**, 1659 (1987).

[28] M. Hillery, Photon number divergence in the quantum theory of n-photon down conversion, Phys. Rev. A **42**, 498 (1990).

[29] S. L. Braunstein and C. M. Caves, Phase and homodyne statistics of generalized squeezed states, Phys. Rev. A **42**, 4115 (1990).

[30] A. Vourdas, Generalized squeezing, Bogoliubov quasiparticles, and information in two- and three-mode systems, Phys. Rev. A **46**, 442 (1992).

[31] D. F. Walls, Squeezed states of light, Nature (London) **306**, 141 (1983).

[32] R. J. Glauber, Coherent and incoherent states of the radiation field, Phys. Rev. **131**, 2766 (1963).

[33] W.-M. Zhang, D. H. Feng, and R. Gilmore, Coherent states: Theory and some applications, Rev. Mod. Phys. **62**, 867 (1990).

[34] C. W. S. Chang, C. Sabín, P. Forn-Díaz, F. Quijandría, A. M. Vadiraj, I. Nsanzineza, G. Johansson, and C. M. Wilson, Observation of three-photon spontaneous parametric down-conversion in a superconducting parametric cavity, Phys. Rev. X **10**, 011011 (2020).

[35] K. Banaszek and P. L. Knight, Quantum interference in three-photon down-conversion, Phys. Rev. A **55**, 2368 (1997).

[36] F. Albarelli, M. G. Genoni, M. G. A. Paris, and A. Ferraro, Resource theory of quantum non-Gaussianity and Wigner negativity, Phys. Rev. A **98**, 052350 (2018).

[37] Y. Zheng, O. Hahn, P. Stadler, P. Holmvall, F. Quijandría, A. Ferraro, and G. Ferrini, Gaussian conversion protocols for cubic phase state generation, PRX Quantum **2**, 010327 (2021).

[38] P. McConnell, A. Ferraro, and R. Puebla, Multi-squeezed state generation and universal bosonic control via a driven quantum Rabi model, arXiv:2209.07958.

[39] W. Ma, S. Puri, R. J. Schoelkopf, M. H. Devoret, S. M. Girvin, and L. Jiang, Quantum control of bosonic modes with superconducting circuits, Sci. Bull. **66**, 1789 (2021).

[40] A. F. Kockum, A. Miranowicz, S. D. Liberato, S. Savasta, and F. Nori, Ultrastrong coupling between light and matter, Nat. Rev. Phys. **1**, 19 (2019).

[41] F. Mei, V. M. Stojanović, I. Siddiqi, and L. Tian, Analog superconducting quantum simulator for Holstein polarons, Phys. Rev. B **88**, 224502 (2013).

[42] V. M. Stojanović and I. Salom, Quantum dynamics of the small-polaron formation in a superconducting analog simulator, Phys. Rev. B **99**, 134308 (2019).

[43] J. K. Nauth and V. M. Stojanović, Spectral features of polaronic excitations in a superconducting analog simulator, Phys. Rev. B **107**, 174306 (2023).

[44] J. Casanova, R. Puebla, H. Moya-Cessa, and M. B. Plenio, Connecting nth order generalised quantum Rabi models: Emergence of nonlinear spin-boson coupling via spin rotations, npj Quantum Inf. **4**, 47 (2018).

[45] W. Yang, Z.-Y. Wang, and R.-B. Liu, Preserving qubit coherence by dynamical decoupling, Front. Phys. **6**, 2 (2011).

[46] J. R. Johansson, P. D. Nation, and F. Nori, QuTiP: An open-source Python framework for the dynamics of open quantum systems, Comput. Phys. Commun. **183**, 1760 (2012).

[47] J. R. Johansson, P. D. Nation, and F. Nori, QuTiP 2: A Python framework for the dynamics of open quantum systems, Comput. Phys. Commun. **184**, 1234 (2013).

[48] B. Vlastakis, G. Kirchmair, Z. Leghtas, S. E. Nigg, L. Frunzio, S. M. Girvin, M. Mirrahimi, M. H. Devoret, and R. J. Schoelkopf, Deterministically encoding quantum information using 100-photon Schrödinger cat states, Science **342**, 607 (2013).

[49] M. Bild, M. Fadel, Y. Yang, U. von Lüpke, P. Martin, A. Bruno, and Y. Chu, Schrödinger cat states of a 16-microgram mechanical oscillator, Science **380**, 274 (2023).

[50] F. Yoshihara, T. Fuse, S. Ashhab, K. Kakuyanagi, S. Saito, and K. Semba, Superconducting qubit-coscillator circuit beyond the ultrastrong-coupling regime, Nat. Phys. **13**, 44 (2017).

[51] F. A. Cárdenas-López and X. Chen, Shortcuts to adiabaticity for fast qubit readout in circuit quantum electrodynamics, Phys. Rev. Appl. **18**, 034010 (2022).

[52] K. G. Johnson, J. D. Wong-Campos, B. Neyenhuis, J. Mizrahi, and C. Monroe, Ultrafast creation of large Schrödinger cat states of an atom, Nat. Commun. **8**, 697 (2017).

[53] B. Hacker, S. Welte, S. Daiss, A. Shaukat, S. Ritter, L. Li, and G. Rempe, Deterministic creation of entangled atom-light Schrödinger-cat states, Nat. Photon. **13**, 110 (2019).

[54] J. Koch, G. R. Hunanyan, T. Ockenfels, E. Rico, E. Solano, and M. Weitz, Quantum Rabi dynamics of trapped atoms far in the deep strong coupling regime, Nat. Commun. **14**, 954 (2023).

[55] C. Monroe, D. M. Meekhof, B. E. King, and D. J. Wineland, A "Schrödinger cat" superposition state of an atom, Science **272**, 1131 (1996).

[56] M. Płodzień, T. Sowiński, and S. Kokkelmans, Simulating polaron biophysics with Rydberg atoms, Sci. Rep. **8**, 9247 (2018).

[57] V. M. Stojanović, Scalable W-type entanglement resource in neutral-atom arrays with Rydberg-dressed resonant dipole-dipole interaction, Phys. Rev. A **103**, 022410 (2021).

[58] D. J. Wineland, Nobel lecture: superposition, entanglement, and raising Schrödinger's cat, Rev. Mod. Phys. **85**, 1103 (2013).

[59] D. V. Sychev, A. E. Ulanov, A. A. Pushkina, M. W. Richards, I. A. Fedorov, and A. I. Lvovsky, Enlargement of optical Schrödinger's cat states, Nat. Photon. **11**, 379 (2017).

[60] J.-Q. Liao, J.-F. Huang, and L. Tian, Generation of macroscopic Schrodinger-cat states in qubit-oscillator systems, Phys. Rev. A **93**, 033853 (2016).

[61] V. Vedral, M. B. Plenio, M. A. Rippin, and P. L. Knight, Quantifying entanglement, Phys. Rev. Lett. **78**, 2275 (1997).

[62] L. Amico, R. Fazio, A. Osterloh, and V. Vedral, Entanglement in many-body systems, Rev. Mod. Phys. **80**, 517 (2008).

[63] I. Bengtsson and K. Zyczkowski, *Geometry of Quantum States: An Introduction to Quantum Entanglement* (Cambridge University, Cambridge, England, 2000).

[64] N. Khaneja, T. Reiss, C. Kehlet, T. Schulte-Herbrüggen, and S. J. Glaser, Optimal control of coupled spin dynamics: design of NMR pulse sequences by gradient ascent algorithms, J. Magn. Reson. **172**, 296 (2005).

[65] N. Wu, A. Nanduri, and H. Rabitz, Optimal suppression of defect generation during a passage across a quantum critical point, Phys. Rev. B **91**, 041115(R) (2015).

[66] C. Whitty, A. Kiely, and A. Ruschhaupt, Quantum control via enhanced shortcuts to adiabaticity, Phys. Rev. Res. **2**, 023360 (2020).

[67] C. Whitty, A. Kiely, and A. Ruschhaupt, Robustness of enhanced shortcuts to adiabaticity in lattice transport, Phys. Rev. A **105**, 013311 (2022).

[68] S. H. Hauck and V. M. Stojanović, Coherent atom transport via enhanced shortcuts to adiabaticity: Double-well optical lattice, Phys. Rev. Appl. **18**, 014016 (2022).

[69] M. Odelli, V. M. Stojanović, and A. Ruschhaupt, Spin squeezing in internal bosonic Josephson junctions via enhanced shortcuts to adiabaticity, Phys. Rev. Appl. **20**, 054038 (2023).